Fizika Nizkikh Temperatur, 1997, v. 23, Nos. 5/6, p. 515–526

Structure and superfluidity of ^{4}He films on plated graphite

J. Nyéki[a], R. Ray, G. Sheshin[b], V. Maidanov[b], V. Mikheev[c], B. Cowan, and J. Saunders

Millikelvin Laboratory, Department of Physics, Royal Holloway University of London, Egham, Surrey, TW20 OEX, U.K.
E-mail:j.saunders@rhbnc.ac.uk

Submitted January 20, 1997

The results of an experimental study using torsional oscillators of the superfluidity of ^{4}He films adsorbed on hydrogen plated graphite are reported. The evolution of superfluidity with the growth of the film shows considerable structure arising from the atomic layering of the film. There is evidence that the superfluidity of a single fluid layer is strongly suppressed, possibly due to the influence of the periodic potential arising from the underlying solid layer. The behaviour of two fluid layers is quite distinct, but shows similarities to that of thicker films on heterogeneous substrates; we suggest that the usual theory of the superfluidity of two-dimensional ^{4}He should be extended to account for superfluid onset temperatures in such a film.

PACS: **67.70.+n**, 67.40.Kh, 67.40.Pm

Dedication

This paper gives a brief survey of one aspect of the results of a research collaboration between scientists from the B I. Verkin Institute for Low Temperature Physics and Engineering in Kharkov and Royal Holloway University of London. This has been made possible by the support of the Royal Society (London) and the Engineering and Physical Sciences Research Council (United Kingdom). In the low temperature experiments reported here samples were cooled using a cryogenic cycle and sorption pumped, dilution refrigerator of the type pioneered by Professor B. N. Eselson and his group. This was initially constructed in Kharkov, modified and developed at Royal Holloway, and provided an excellent low mechanical noise environment for these studies involving sensitive, high Q, mechanical oscillators. Further developments and the commercialization of this refrigerator technique are described elsewhere in this volume. This paper is intended as a tribute to the memory of Professor B. N. Eselson and the tradition of low temperature helium research at Kharkov to which he contributed so significantly.

1. Introduction

The superfluid transition of a thin ^{4}He film on a planar surface is understood in terms of a Kosterlitz-Thouless (KT) two-dimensional phase transition [1]. Above some critical temperature vortex-antivortex pairs become unbound, the film cannot support a superflow and the superfluid density drops discontinuously to zero. Clear confirmation of these ideas was primarily due to the experiments of Reppy and co-workers, at Cornell [2]. They adsorbed the helium film on a sheet of mylar, contained inside a torsional oscillator. Associated with the superfluid transition of the film is a shift in the period of the oscillator, resulting from the drop in its effective moment of inertia as the film decouples from the substrate. This method was a development of that first used by Andronikashvili [3] to deter-

[a] Permanent address: Institute of Experimental Physics, Slovak Academy of Sciences, Kosice, Slovak Republic.
[b] Permanent address: B. I. Verkin Institute for Low Temperature Physics and Engineering, National Academy of Sciences, Kharkov, Ukraine.
[c] Permanent address: Oxford Instruments plc, Eynsham, U.K. Former address: B. I. Verkin Institute for Low Temperature Physics and Engineering, National Academy of Sciences, Kharkov, Ukraine.

mine the superfluid density of bulk liquid ^{4}He. The key features of the Cornell torsional oscillators were their high quality factor $Q \geq 10^5$, and a typical frequency in the range 0.5–2 kHz outside that of most vibrational noise on a typical cryostat. This technique allowed the resolution of the small period shifts due to the superfluid transition in the film (typically of order nanosecond compared to a period of order 1 ms) as well as a characteristic dissipation peak at the superfluid transition. The discontinous period jump predicted by KT is somewhat rounded by the finite frequency at which the superfluid response is measured. However it was possible to confirm the universal relation for the jump $\rho_s(T_c)/T_c = 2m^2k_B/\pi\hbar^2$. A comparison of results with the dynamic KT theory can be found in Agnolet, McQueeney and Reppy (AMR) [4].

The mylar substrate used in this early work is extremely heterogeneous, i.e. the substrate is disordered, due to atomic scale roughness. One consequence of this is that, up to some threshold coverage, the helium film is localized and no superfluid transition is observed. This threshold coverage is commonly referred to as the «dead layer» or «inert layer». It has been suggested that superfluid onset, as a function of coverage at $T = 0$, may be regarded as a transition between an insulating disordered (Bose glass) phase and superfluid [5].

Recently attention has turned to the study of ^{4}He films adsorbed on the basal plane of graphite using these sensitive torsional oscillator methods. The first such study of superfluidity in this system was performed by Crowell and Reppy (CR) [6], while Mohandas et al. [7] concentrated on submonolayer films and found no evidence for superfluidity in these. Exfoliated graphite substrates were used to provide a sufficiently large surface area to allow measurements of adequate sensitivity. It is well established that this substrate consists of atomically flat crystallites of typical dimension a few hundred Angströms and thus provides a homogeneous binding potential for the adsorbate. Residual heterogeneity, at the crystallite edges, localizes about 2% of the first helium layer, and so is a relatively weak effected. The important point is that, on this substrate, the film is atomically layered; clear periodic structure has been seen in the compressibility of the film, as determined from vapour pressure adsorption isotherms [8], as well as in the heat capacity [8,9] and third sound velocity measurements [8]. Layering of the film is also seen in first principles calculations of the film structure [10]. Thus in contrast to heterogeneous substrates the structure of the film is, in principle, well defined. This structure turns out to have a profound influence on the development of superfluidity.

Exfoliated graphite substrates have been widely used in the study of adsorbed gases [11]. In principle it is possible to modify the surface binding potential, in a reasonably controlled and well characterized way, by preplating with either an inert gas or hydrogen. The objective is to coat the graphite with an integral number of atomic layers of the preplating gas, to provide a composite substrate of weaker binding potential. This binding potential can be varied from that of bare graphite to that of the preplating material for a sufficiently thick film, so long as it wets the graphite surface. This is the approach used in the present work, where we have plated the graphite with a bilayer and a trilayer of HD. Here the use of HD, rather than H_2 or D_2 is because of absence of any ortho-para conversion and associated heating at ultralow temperatures.

Our use of hydrogen plating is also motivated, in part, by previous studies of the superfluidity of ^{4}He on hydrogen films. The expected advantage of using a thick hydrogen film as substrate was to avoid solidification of the first ^{4}He layer, offering the prospect of observing superfluidity in a submonolayer ^{4}He film. Brisson et al. [12] studied third sound propagation in helium films adsorbed on hydrogen plated glass, while Mochel and coworkers [13] and Adams and Pant [14] have investigated helium on metallic surfaces plated with thick hydrogen films using third sound and torsional oscillators, respectively. These last two studies indeed give evidence of submonolayer superfluidity of the ^{4}He film. In addition Mochel and Chen [13] found evidence for a second transition below the superfluid transition and also observed two third sound modes under certain conditions.

Although these experiments rely on the formation of a uniform hydrogen film, it is in fact not clear that hydrogen wets metallic substrates, indeed there is some clear experimental evidence to the contrary [15]. Thus the philosophy behind the present experiment was to start with well characterized thin hydrogen films, up to three atomic layers, adsorbed on graphite. The structure of such films has been investigated by neutron scattering and their density determined [16], so it is established that they wet the surface. The goal to grow a thick hydrogen film on graphite remains a challenge for the future. The first study of the superfluidity of ^{4}He on hydrogen plated graphite was the third sound measurements of Zimmerli, Mistura and Chan (ZMC) [8]. Heat capacity measurements have also been performed by Vilches and co-workers [17], provid-

ing valuable insights into the structure of the ^{4}He film.

One disadvantage of the exfoliated graphite substrate is that, on length scales greater than of order 1 μm, it is extremely disordered. This results in a tendency for the superfluid film to be entrained by the oscillator, so that the full period shift due to the onset of superfluidity is not observed. This effect is parameterized by a quantity, conventionally referred to as the χ factor, reflecting the fraction of superfluid which does not decouple from the surface. For mylar [4] $\chi \sim 0.14$, while for Grafoil CR [6] found $\chi = 0.989$, reflecting the poor connectivity of the surface. The present work gives a value around 0.95 depending on the preplating (see Sec. 3.4) for more detail). However, although these χ factors are relatively close to unity, tending to reduce the observed period shifts due to superfluidity, this is compensated by the large specific surface area of the substrate.

A broad overview of the growth of helium films on graphite is as follows. The submonolayer film has a rich phase diagram that has been characterized by heat capacity [18] and neutron scattering measurements [19]. At the coverage at which a second layer begins to form (second layer promotion) the first layer consists of an incommensurate solid on a triangular lattice [20]. At third layer promotion the second layer is also solid at sufficiently low temperatures [9]. Subsequent layers are fluid; thus only two layers solidify on bare graphite. In the present work we have preplated the graphite by a bilayer and a trilayer of HD. In contrast to bare graphite, it appears that in this case only one helium layer solidifies, due to the weaker binding potential of the preplated graphite surface. Note that, as previously mentioned, it is believed that for a bulk hydrogen surface the binding potential is sufficiently weak that the first helium layer should not solidify [21].

A further important detail concerns the evolution of the fluid layers. Consider the second layer on bare graphite, which at low densities is fluid (the layer begins to solidify around 5.5 nm^{-2}). Theory predicts that, at sufficiently low temperatures, this fluid is self-condensed [22] with a density of roughly 4 nm^{-2} and this is supported by measurements of the heat capacity [9]. On cooling, at second layer coverages less than 4 nm^{-2}, it is therefore expected that the second layer fluid first phase separates into a low density «gas» and a high density «fluid». (At $T = 0$ the density of the «gas» component vanishes and that of the fluid is of order 4 nm^{-2}.) Following phase separation, the superfluid transition subsequently occurs in the high density liquid component. Thus, in this case, superfluid onset will be controlled by the intersection in the temperature-coverage plane of the boundary of the 2*D* gas-liquid coexistence region and the line of superfluid transitions of a uniform fluid film [23, 24]. Intriguingly, Clements et al. [25] found such a coexistence region in each of the first three fluid layers on bare graphite, or layer by layer condensation. The possible interplay between such phase transitions in the film and its superfluidity is an important factor in the interpretation of these experiments.

The organization of this paper is as follows. A brief description of the experimental method is given in Sec. 2, including details of the torsional oscillator, the *in situ* pressure gauge for sample characterization and the method of data collection. Section 3 contains the main experimental results together with their interpretation. Although the observed behaviour is rich in detail, we believe the systematics of the interplay between superfluidity and film structure emerge quite clearly. For clarity this section is split into a number of subsections dealing with the method adopted to preplate the graphite with a bilayer or trilayer of HD (3.1), the characterization of the growth of the ^{4}He film on these preplated substrates by vapour pressure adsorption isotherms (3.2). There follows the longest subsection (3.3) describing the evolution of superfluidity in the first two fluid layers. These results appear to show that a periodic potential strongly suppresses superfluidity and that the superfluid transition of two fluid layers is no longer described by Kosterlitz–Thouless theory in its simplest form. In subsection (3.4) we discuss our determination of the χ factor of the substrate. A number of further interesting experimental observations are collected in (3.5), including features which may signify the layer by layer condensation in the film, the observation of periodicity of the third sound speed and a coverage dependence of the vortex dynamics. Section 4 summarizes the main conclusions of the paper, with suggestions for future work.

2. Experimental method

The torsional oscillator is of conventional design, consisting of a stycast 1 266 shell, of internal diameter 18 mm and height 12 mm, packed with Grafoil and mounted on a hollow BeCu torsion rod. The torsion mode or floppy mode are driven and detected capacitatively. The frequencies are 1 056 and 605 Hz, respectively. The device is operated in a self-resonant oscillator circuit, at constant drive

voltage, with the torsional oscillator as the frequency determining element. The period of the oscillator is measured with a HP5335A counter. The response of the oscillator is preamplified, and then lockin detected. The amplitude of oscillations is proportional to the quality factor of the oscillator, and is calibrated by observing the ring down of the oscillator on removing the drive.

The Grafoil sample is in the form of discs 0.15 mm in thickness, providing a total surface area of 65 m^2. It was baked in vacuum at 1100 °C to remove impurities, before loading it in the cell. It is necessary to measure the background period and dissipation of the oscillator as a function of temperature between 12 K and 20 mK. These are smooth with no anomalous features. When the adsorbed film is not superfluid the torsional oscillator simply acts as a sensitive microbalance, with period shift proportional to the coverage (mass) of the adsorbed film. For our oscillator the sensitivity with respect to the areal density of the ^{4}He film is 26 ns·nm^2.

The cell is attached via a massive vibration isolator to a cell plate which is in turn connected to the mixing chamber of a cryogenic cycle, sorption pumped, dilution refrigerator [26] via a weak thermal link. This enables the temperature of the cell to be swept slowly, using a heater attached to the cell plate, to accumulate period and dissipation data. The sweep rate is such that there is negligible hysteresis between data taken on warming and cooling. The temperature is measured by a 470 Ω Speer resistor and a GaAs chip resistor [27], calibrated by a ^{3}He melting curve thermometer between 0.05 and 0.8 K and by a calibrated germanium resistance thermometer between 0.3 and 4 K.

An *in situ* pressure gauge similar in design to that used by Zummerli [28] and by Crowell [6] was connected to the cell and mounted on the cell plate. The deflection of the gold plated kapton membrane was detected capacitatively and yielded a pressure resolution of 5 nbar. The reference volume of this gauge was connected by a capillary to room temperature for rough evacuation, a small pill of graphite inside the reference volume ensured a good vacuum at low temperatures and provided a better reference pressure than simply connecting one side of the diaphragm to the vacuum can (in our case this was pumped by a graphite cryopump attached to the 1 K pot). The gauge was calibrated against the vapour pressure of liquid ^{4}He (actually a thick ^{4}He film of 20 layers in the torsional oscillator), over the temperature range 0.75 to 1.25 K. This gauge was used for vapour pressure adsorption isotherms to characterize the growth of the HD preplating film and the ^{4}He film. In addition the *in situ* gauge monitored the vapour pressure of the film during collection of period data, enabling corrections to be made to the oscillator period due to desorption of the film at higher temperatures. The system was also equipped with a room temperature Paroscientific pressure gauge [29].

The cell fill line was equipped with a series of heaters needed when preplating the graphite with hydrogen, both during the performance of isotherms (at 12 and 10 K) and when cooling the cell to 4.2 K, to ensure that the cell is the coldest point thus avoiding the formation of bulk hydrogen in the fill line. The period of the torsional oscillator, effectively acting as a microbalance, provides an extremely sensitive detector of any unwanted loss of hydrogen from the cell.

3. Results

3.1. Preplating with HD

Measurements on ^{4}He films were made with preplatings of a bilayer and a trilayer of HD. The procedure for determining these preplatings was as follows. The surface area of the sample was determined by a 4.2 K ^{4}He isotherm, taking point *B* [18] as the indicator of first layer promotion. We use this as the reference for all surface densities in this paper. The density of H_2 and D_2 films on graphite (one, two and three layers) have been measured by neutron scattering [16]. With this information and the bulk molar volume we generate the density per layer as a function of the reciprocal number of layers. These data can be interpolated to estimate the values for HD films, with a precision of order 2% (18.3 and 27.1 nm^{-2} for bilayer and trilayer, respectively). Scaling the dose for ^{4}He monolayer completion by the ratio of these densities and the neutron scattering density of a completed ^{4}He monolayer (11.25 nm^{-2}) [20], gives the estimated required dose for a bilayer or trilayer of HD.

Further we have performed a HD vapour pressure isotherm at 12 and 10 K and found compressibility minima in good agreement with these estimates (corresponding to densities 18.9 and 27.2 nm^{-2} for the bilayer and trilayer). The preplating coverages chosen were those corresponding to these compressibility minima [30]. Following these procedures we can be confident that the chosen preplatings are very close to exactly two and three layers.

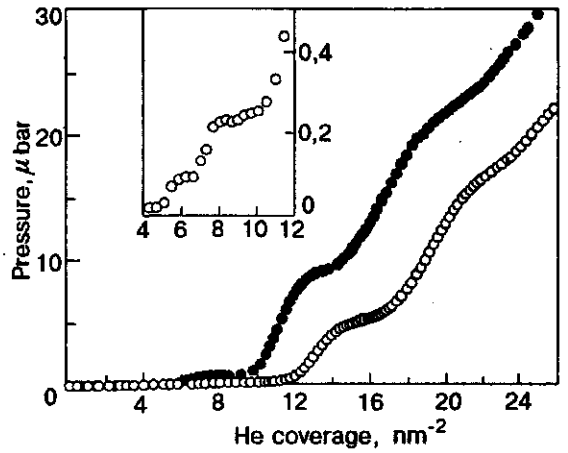

Fig. 1. ^{4}He vapour pressure isotherms, taken at 940 mK, for graphite plated with a bilayer (open circles) and trilayer (filled circles) of HD. Inset shows detail for bilayer preplating, near first layer promotion. Structure is believed to arise from solidification of film, followed by promotion at 7.3 nm^{-2}.

3.2. Characterization of ^{4}He film

For each HD preplating case a helium isotherm was performed to characterize the growth of the film, locating the layer promotions. Results for the bilayer and trilayer preplating of isotherms at 940 mK are shown in Fig.1. Layer promotions were determined from compressibility minima, and a ^{4}He coverage scale defined. These coverages are referred to the 4.2 K ^{4}He isotherm on bare graphite, for which first layer promotion is taken as 11.4 nm^{-2}. For the bilayer preplating these promotions occur at 7.3, 12.5, 18.7 and 25.2 nm^{-2}. The last three values are all 20% smaller than obtained by ZMC for ^{4}He on graphite preplated by a bilayer of hydrogen, thus our coverage scales are consistent within a constant scaling factor. For the trilayer preplating we find shifted compressibility minima at 5.65, 10.3, 16.7, 24.0 nm^{-2}. Most of the coverage offset between these two isotherms for different preplatings is attributable to a significantly lower density of the first ^{4}He layer for the trilayer preplating.

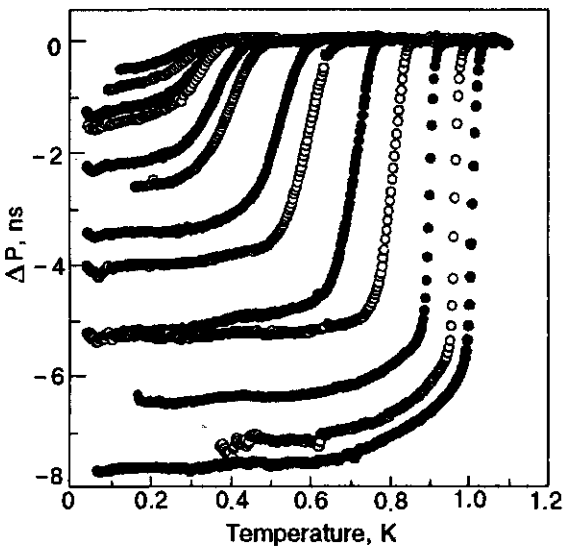

Fig. 2. Period shift due to superfluid transition for trilayer preplating. Coverages: 7.02, 7.50, 8.15, 8.47, 9.11, 9.35, 9.61, 9.74, 10.16, 10.60, 11.71, 12.58, 13.11 nm^{-2}.

For both preplatings no superfluid signature is observed from the first ^{4}He layer fluid, at lower coverages. This layer is believed to be solid on completion. The low density of second layer promotion for the trilayer preplating may arise from a registered structure which resists compression. In the following we will assume that the first layer is solid; the second and third layers are thus the first and second *fluid* layers. The development of superfluidity in these fluid layers is discussed in the next subsection.

We should note that CR detected superfluidity in the second layer of ^{4}He on bare graphite prior to solidification, the period shifts associated with superfluidity having an anomalous temperature dependence. According to the phase diagram of Greywall [9] these superfluid transitions occur when the film is a coexistence of gas and liquid. This may be responsible for the anomalous behaviour observed. For the present case of HD preplated substrates we currently believe that the observation of superfluidity in the first ^{4}He layer is precluded by the solidification of the film, which in this case occurs at lower second layer coverages. On the basis of experiments on ^{3}He films on a HD bilayer preplated graphite substrate, we expect to enter a commensurate solid-fluid coexistence region at 4.8 nm^{-2}, in the low-temperature limit [31].

3.3. Evolution of superfluidity in the first two fluid layers

Results for the period shift due to the superfluid transition and the associated dissipation peak are shown for a selection of lower coverages for the trilayer preplating [32] in Figs. 2, 3. The temperature dependence of the period shift for the three highest coverages, just after formation of the second fluid layer, are most characteristic of a KT transition. The dissipation peak associated with the transition is relatively narrow, with temperature halfwidth of order 30 mK. For each coverage these data allow us to determine the total period shift due to the onset of superfluidity $\Delta P(0)$. This quantity is the difference between the estimated $T = 0$ limit of

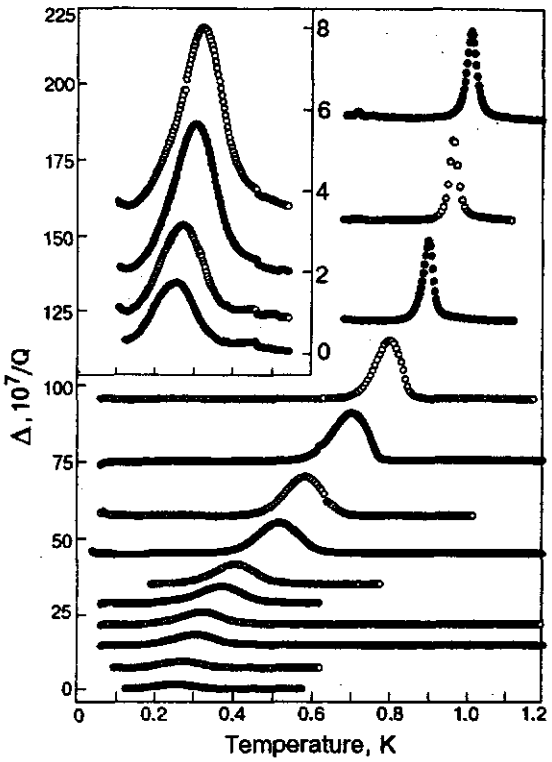

Fig. 3. Dissipation peaks at the superfluid transition, with trilayer preplating. Coverages are the same as for Fig. 2. Data is displaced for clarity. Inset shows data for the first four coverages on an enlarged scale.

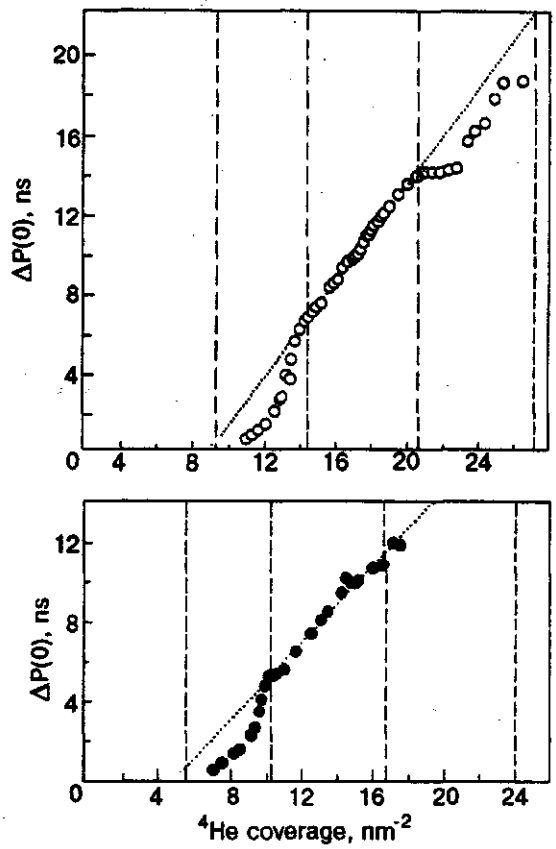

Fig. 4. Total period shift as a function of coverage. Upper plot (open circles); bilayer preplating. Lower plot (filled circles); trilayer preplating. Vertical dashed lines indicate coverages of layer promotions, inferred from vapour pressure isotherms. Dotted line is a linear fit to period shift data in the third layer (second fluid layer).

the period and the period immediately above the superfluid transition, after applying the vapour pressure correction. These data are plotted as a function of the total ^{4}He coverage in Fig. 4. Values of T_c, here defined as the temperature of the dissipation maximum, are shown in Fig. 5.

3.3.1. First fluid layer. It can be seen that the behaviour is rather similar for the two preplatings, apart from a coverage shift referred to earlier, and attributed to differences in density of the first solid layer. The behaviour in the second ^{4}He layer (first fluid layer) is very similar to that observed in the third layer (again first fluid layer) by CR on bare graphite. We interpret the break in the coverage dependence of $\Delta P(0)$ and T_c, part way through filling of the fluid layer as due to the two dimensional condensation («puddling») of that layer at lower coverages, as previously proposed by CR. Thus up to a total coverage 10.8 (9.3) nm^{-2} for the bilayer (trilayer) preplating, the fluid layer separates on cooling into a low density «gas» and high density «liquid». The superfluid transition observed is that of the high density «liquid» component. The break then corresponds to the point in the T–n-plane at which a line of superfluid transitions

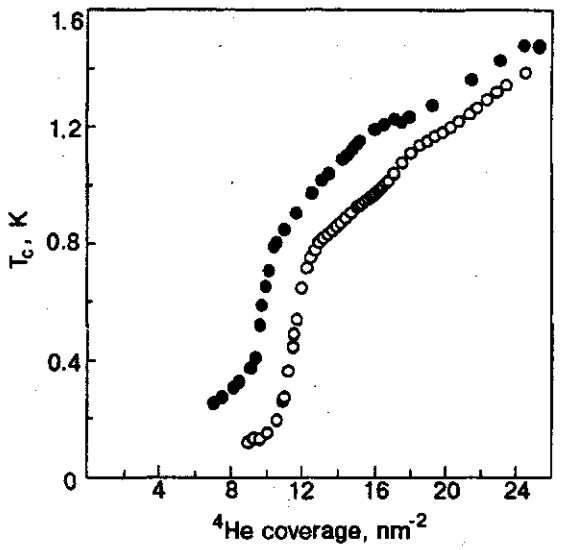

Fig. 5. Temperature of dissipation peak, used to locate superfluid transition temperature, as a function of coverage. Open circles; bilayer preplating. Filled circles; trilayer preplating.

emerges from the two-phase coexistence regime. These results are broadly consistent with third sound measurements of ZMC [8] on H_2 plated graphite, which also find superfluidity in the second ^4He layer.

Recent heat capacity measurements on this system [17], with preplatings slightly in excess of exact bilayer and trilayers of hydrogen, also provide evidence of such a layer condensation, with a critical temperature of 0.8 K. From our data, for both preplatings, we estimate the minimum density of the second layer fluid at which a uniform fluid is stable to $T = 0$ to be $n_2 = 4 \pm 0.5$ nm^2, where the error largely comes from uncertainties in the precise density of the first solid layer. This is in reasonable agreement with the theory [22, 25].

Examination of the period shift curves for the four coverages studied below the break for the trilayer preplating (Fig. 2), shows that «superfluid onset», now defined as the temperature at which a shift in period is first resolved, occurs at the same temperature, ~ 0,4 K, at each coverage. Similar behaviour is seen for the bilayer preplating. This observation supports the model of a superfluid transition occurring in puddles of condensed liquid, whose density remains constant as a function of coverage. Note that the values of T_c plotted in Fig. 5 are the temperatures of the dissipation maxima and do show a coverage dependence in this regime. This is simply attributable to changes in the temperature width of the superfluid transition. The decrease in width of the transition as the coverage is increased may be associated with the increasing size of the puddles or associated with the effects of percolating superflow between puddles.

We cannot be sure of the morphology of these superfluid puddles but our results suggest that they decouple from the substrate. Either the high density component forms in a single patch, perhaps at the edge of a Grafoil platelet or it is not necessary for superfluid patches to percolate in order to slip relative to the surface. Thus while it is clear that percolation is necessary for dc superfluid mass transport it might be expected that torsional oscillator will continue to detect superfluidity, even if the liquid separates into a set of non-percolating patches.

At higher fluid layer coverages, above the break, in the regime where we expect a uniform fluid layer, there is a rapid increase in both T_c , and $\Delta P(0)$. For both preplatings, this continues until the formation of a second fluid layer. At this point, third layer promotion, there is a second break in the coverage dependence. Similar behaviour was seen on bare graphite by CR [6]. We interpret this data immediately prior to third layer promotion (formation of second fluid layer) as follows. If, in Fig. 4, the line of period shifts (following the break indicating emergence from the coexistence region), is extrapolated to zero, this determines the density at which the onset of superfluidity might be expected for a uniform fluid layer. The line of transition temperatures extrapolates to essentially the same coverage. These are 10.5 nm^{-2} and 8.5 nm^{-2} for the bilayer and trilayer, respectively, and we interpret these as the «dead layer» prior to third layer promotion. Clearly superfluid onset as a function of coverage is not directly observable because of the intervention of 2*D* condensation. This is schematically illustrated in Fig.6. We believe that this suggests that superfluidity is suppressed in the uniform two-dimensional fluid. For both preplatings the extrapolated fluid density, corresponding to the «dead layer» coverage, is 3 nm^{-2}.

This value is comparable to that obtained from third sound measurements on a (nominally) thick hydrogen film by Shirron and Mochel [13] (this gives a dead layer of 3.9 nm^{-2}, after scaling their surface densities by a factor 1.67 as suggested by Cheng et al. [33]). Torsional oscillator measurements on a thick H_2 film [14] give a dead layer of order 1/2 «layer». Note that in the present experiment we have a high degree of confidence in the quality of the surface. In the present measurement, for both bilayer and trilayer preplatings, the apparent inert layer corresponds to of order 0.6 the

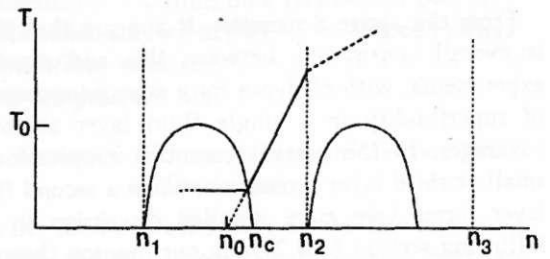

Fig. 6. Schematic diagram to illustrate proposed interplay of superfluidity and 2*D* condensation phenomena. Layer promotions occur at n_1 , n_2 , n_3 . At n_1 the first layer is solid. For $n_1 < n < n_c$, the second layer consists of a self-condensed fluid – gas coexistence. For $n_c < n < n_2$ the second layer is a uniform fluid. After promotion to a third layer at n_2 the third layer fluid is also self-condensed, as suggested in [25]. Critical temperature of both gas–liquid coexistence regions is T_0 , probably of order 0.8 K. A line of superfluid transition temperatures T_c is also shown; T_c is constant in the coexistence region and on entering the uniform fluid phase increases with coverage faster than the KT slope, extrapolating to zero at n_0 (dead layer). There is a break in the coverage dependence of T_c at promotion, $n = n_2$.

density of the fluid layer at promotion plus the first solid layer. One might refer to the fluid component of this inert layer as «nontrivial». The results of CR, on bare graphite, are consistent with these observations.

Over the coverage range under consideration, corresponding to a uniform fluid layer prior to promotion, the increase of T_c with coverage is significantly faster than the KT line $T_c = 0.156\ n$ (K·nm^2). This relation assumes $\rho_s(T_c) = 0.82\ \rho_s(0)$ [2] and assumes the bare mass of the ^{4}He atom. The width in temperature of the dissipation peak at the superfluid transition also decreases rapidly with increasing coverage.

The origin of this strong suppression of superfluidity and the rapid increase in T_c with increasing coverage remains open to question. It may arise from residual heterogeneity of the surface; however the observed behaviour is rather similar for both preplatings reported here and for bare graphite. Rather the observations may indicate the influence of the periodic potential of the underlying solid layer on superfluid onset. The rapid increase in T_c may be associated with the film becoming more delocalized normal to the surface; theory suggests [25] that such an effect can occur at a coverage significantly lower than that of layer promotion.

Note that, although we refer to this fluid layer as being uniform, we expect on the basis of Monte-Carlo simulations of a ^{4}He monolayer on hydrogen [34], that the local density will show structure arising from the periodic surface potential. These simulations show an effective ^{4}He mass up to twice that of the bare mass and a 20% suppression in the superfluid density, as well as condensation below 4.6 nm^{-2}.

From the above discussion, it appears that there is overall consistency between this and previous experiments, with evidence for a strong suppression of superfluidity in a single fluid layer at lower coverages. In the present case this suppression is small at third layer promotion, when a second fluid layer forms (see more detailed discussion in the following section (3.3.2)). In our opinion theoretical work on the influence of the periodic potential on the superfluidity of a single fluid layer, taking into account the delocalization of the film normal to the substrate, would be of great interest.

3.3.2. Two fluid layers. At a coverage of 12.5 (10.3) nm^{-2} for the bilayer (trilayer) preplating the third layer forms. We now have two fluid layers atop a solid ^{4}He layer atop the preplated graphite substrate. The coverage dependence of both T_c and $\Delta P(0)$ show a sharp break at this third layer promotion, for both preplatings. As the third layer (second fluid layer) grows the total period shift $\Delta P(0)$ increases linearly with coverage to a good level of accuracy, $\Delta P(0)$ is a measure of the mass of the film participating in the superfluidity in the $T = 0$ limit. A linear fit to this period data over this coverage range extrapolates to zero at a coverage of 6.7 (4.8) nm^{-2} for the bilayer (trilayer) preplating. In both cases this is close to, but somewhat smaller than, the coverage at which second layer promotion was observed: 7.3 (5.65) nm^{-2}.

This is powerful evidence that, in the low-temperature limit, the film now consists of two superfluid layers atop a solid ^{4}He layer. *All* of the fluid participates in the superfluidity; *the «dead» layer is merely the first solid layer.* This contrasts with the nontrivial dead layer we have argued for in the first fluid layer and is clear evidence for a shift in the density of the inert layer as a function of the coverage of the film.

If a line of transitions with the KT slope is drawn on Fig. 5, $T_c = 0.156\ (n - n_{dead})$ with $n_{dead} = 6.7\ (4.8)$ nm^{-2} for the bilayer (trilayer) preplating, the transition temperature is closest to that observed just at third layer promotion, as the second fluid layer forms. Indeed, for the trilayer preplating the line almost coincides with the data at this point. This therefore suggests that at third layer promotion the first fluid layer is completely superfluid, in marked contrast with the situation at somewhat lower coverages.

The behaviour of ^{4}He on bare graphite as a second fluid layer forms (corresponding to fourth layer promotion in that system) is somewhat more complex. (Clearly in comparing the evolution of superfluidity in the two systems it is the number of fluid layers that is important, this is $l - 2$ for bare graphite and $l - 1$ for preplated graphite, where l is the total number of layers.) The results of CR for T_c and ΔP show a plateaux in the vicinity of third layer promotion, possibly attributable to a reconstruction of the film. We see a similar feature at fourth layer promotion for the bilayer preplating, see Sec. 3.5. The absence of such an effect in the present experiment as the second fluid layer forms simplifies the interpretation.

It is interesting to compare the coverage dependence of T_c with that observed for ^{4}He on mylar [2,4]. In this case the «dead layer» is typically in the range 25–30 μmol·m^{-2}. A simple picture is that this is in the form of an amorphous coating of the substrate, which screens the heterogeneous substrate potential such that additional ^{4}He atoms are delocalized. These fluid atoms undergo a superfluid transition via the KT mechanism; the data of

Bishop and Reppy [2] show a linear T–n dependence, well described by the KT relation $T = 0.156\ n\ (\text{K·nm})^2$. AMR [4] report data over a wider coverage range. In this case the dead layer is 28 μmol·m^{-2}; the initial T–n relation is again reasonably consistent with the KT line. However around 40 μmol·m^{-2}, corresponding to a fluid density of 7 nm^{-2}, the slope of the T–n line decreases. Above 40 μmol·m^{-2} AMR find the slope of the T–n line to be 0.071 K·nm^2. This behaviour is reminiscent of the sharp decrease in dT_c/dn on formation of a second fluid layer in the present hydrogen preplated graphite experiment. In all cases this occurs at $T_c \sim 0.8$ K. It is intriguing, and we believe significant, that for both preplatings we have investigated, T_c increases linearly with coverage as the second fluid layer fills with a slope quite close to that seen on mylar (0.084 K·nm^2 and 0.060 K·nm^2 for trilayer and bilayer preplating respectively).

This suggests that the transition in behaviour is a direct result of the formation of two fluid layers. According to this view the coverage dependence of T_c above promotion is an intrinsic feature of the superfluid transition in two coupled fluid layers. On the mylar substrate the film is not so highly layered, so in this case a sharp kink in the T–n curve is not observed, rather a more gradual but still pronounced change in slope.

In contrast, below this feature, for just one fluid layer, the behaviour is entirely different for the two substrates. The mylar substrate, screened by the ^{4}He inert layer, provides a disordered potential, there is no *2D* condensation of the fluid, and the transition temperature follows the KT line. By contrast the atomically flat plated graphite substrate provides a periodic potential. At fluid coverages below of order 4 nm^{-2} the uniform fluid is unstable at sufficiently low temperatures and 2*D* condensation occurs. Above this coverage there is a strong suppression of both the superfluid transition temperature and the superfluid density, possibly due to the influence of the periodic potential due to the solid underlayer. These results challenge our understanding of superfluidity in helium films and hopefully will stimulate more theoretical work.

3.4. Determination of χ factor

We now discuss measurements of the χ factor of the surface. This is obtained from an isotherm of the oscillator period as a function of coverage, taken at the same time as the vapour pressure isotherm. This filling curve data refers to fully annealed films; this procedure was possible because of the good long term stability of the cell period. (An alternative is to fill the cell at constant temperature, which can lead to non-uniform coverages.) Results for the trilayer are given in Fig.7. In this case the superfluid transition temperature at the temperature of the measurement is around 12 nm^{-2}. A linear fit to data below 11 nm^{-2} (normal film at this temperature) gives a mass sensitivity of 26.01 ns·nm^2. For coverages above 13 nm^{-2} for which the film is superfluid, a linear fit gives a slope of 25,014 ns·nm^2. This gives a χ factor of 0.9617. For the bilayer preplating we obtain a normal mass sensitivity of 26.00 ns·nm^2, in excellent agreement with the trilayer result. In this case the χ factor is 0.9519. With this data the expected slopes of the $\Delta P(0)$ vs. n lines after third layer promotion are 1.25 (0.995) ns·nm^2 for the bilayer (trilayer) preplating. These values compare quite well to those obtained from Fig. 4, 1.176 (0.949) ns·nm^2. It is possible that the superfluid fraction at $T = 0$ is suppressed in these films, but this cannot be measured directly as it cannot be separated from the effects represented by the χ factor. CR report a χ factor of 0.989 for ^{4}He on bare graphite. For our Grafoil sample with no preplating we find $\chi = 0.956$, a result obtained from a filling curve on bare graphite in the same cell following the same procedures. It therefore seems that the preplating does not have a big effect on the χ factor, and it is likely that most of the difference between our result and that of CR arises from details of substrate quality or the effects of different heat treatment.

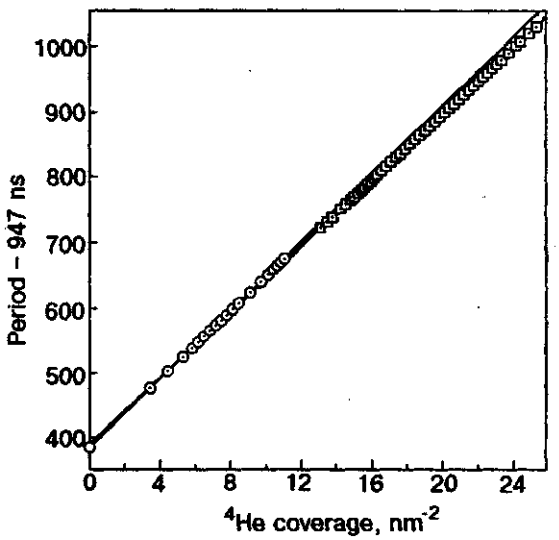

Fig. 7. Determination of χ factor. ^{4}He filling curve at 940 mK (for trilayer preplating), showing change in period as a function of coverage. Circles: non-superfluid coverages. Squares: superfluid coverages. Linear fit to each of these sets of data are shown. Results in vicinity of superfluid transition are omitted from analysis.

3.5. Other experimental features

In the third layer (second fluid layer) for bilayer preplating, we find a set of small steps in the period data, associated with small and sharp peaks in the dissipation. Because we have studied a large number of closely spaced coverages we can follow the evolution of this feature. The locus in the T–n plane is shown in Fig. 8, and is suggestive of that of a two phase coexistence region, or layer by layer fluid condensation as predicted by Clements et al. [25]. Thus in this region the second layer would be a uniform fluid and the third layer puddled. The width of the coexistence region is 4 nm^{-2} and the critical temperature of 0.8 K is close to that found from heat capacity measurements in the second layer. We emphasize that this attribution is extremely tentative.

We should point out that in this coverage regime the period shift and amplitude data suffer from contamination by third sound resonances [35]. These could be eliminated in an oscillator with lower operating frequency. Driving the oscillator in its floppy mode helps to separate out third sound resonances. However we can exploit the observed mode crossings, the most pronounced signature of which is dramatic decrease in the Q factor of the torsion mode, to trace the evolution of the third sound velocity. For the bilayer preplating the temperature of the mode crossing exhibits a maximum at 16.7 nm^{-2}; this arises from a compressibility minimum in perfect agreement with that determined from the vapour pressure isotherm locating third layer promotion, as expected. In contrast, the measurements of ZMC [8] show a coverage offset between maxima in the third sound velocity and compressibility minima. This may arise because the measurements are dominated from different graphite surfaces in the same cell. The velocity data comes from a cleaved highly oriented pyrolytic graphite (HOPG) crystal while that for the vapour pressure is dominated by the graphite foam ballast in the same cell.

Above fourth layer promotion (formation of the third fluid layer) the bilayer preplating period shift data shows a plateau of width 2.5 nm^{-2}. Additional ^{4}He atoms added to the film appear not to contribute to the superfluidity. This most likely arises from a reconstruction of the film, involving an increase in the density of the first solid layer. A similar plateau of comparable width was seen by CR, also at fourth layer promotion, which in this case corresponds to the formation of the second fluid layer. These authors suggested a number of possible explanations for such structure in the period shift isotherms, including that of film reconstruction just mentioned. It seems that the absence of a plateau in the present data above third layer promotion should add extra constraints on the possible explanation of such features. On the one hand, it appears to favour less strongly the model of Zimanyi et al. [36], who calculate the superfluid density in Bose-Hubbard model. On the other hand we do not believe that the plateaux can arise from puddling, one of the possibilities suggested in [6] and by Clements et al. [25], since we observe a linear dependence of ΔP on coverage in the second fluid layer. Puddling is predicted in this layer, and as discussed we have signatures in the torsional oscillator response which can tentatively be ascribed to the onset of puddling.

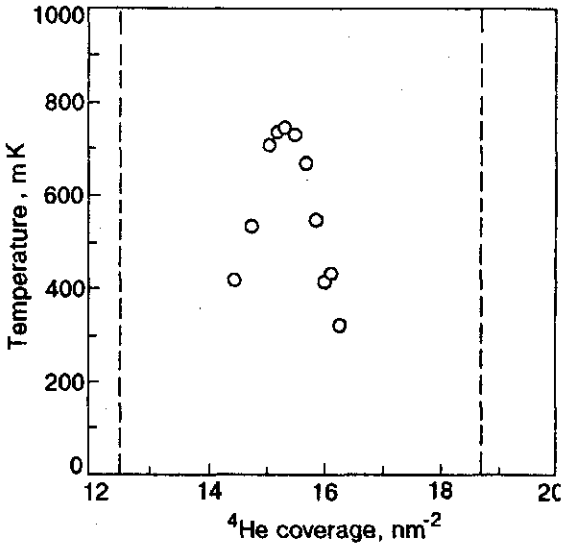

Fig. 8. Locus in T–n plane of features in oscillator (small period step, sharp peak in dissipation) tentatively associated with puddling transition in third layer.

Another striking feature of the evolution of superfluidity concerns the width of the dissipation peak at superfluid onset. Thus should be sensitive to the vortex dynamics in the film. For both preplatings the data show a rather similar coverage dependence, Fig. 9. Following the end of second layer puddling the peak halfwidth decreases dramatically, through third layer promotion. As the next fluid layer (third layer) fills, the dissipation exhibits a minimum, around 0.3 layer filling, followed by a maximum, around 0.7 layer filling for both preplatings. Since as the third layer fills, the superfluid transition temperature exceeds 0.8 K, above the critical temperature for gas-liquid coexistence, both the second and third fluid layers should be uniform fluids at superfluid onset, so there should be no effect of puddling on the dissipation near onset.

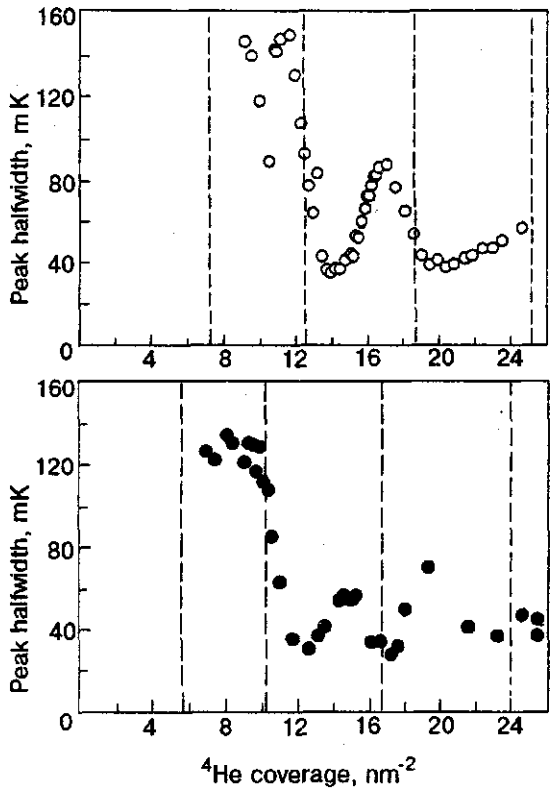

Fig. 9. Coverage dependence of width of superfluid transition. Temperature halfwidth of dissipation peak at superfluid transition plotted as a function of coverage. Open (filled) circles are for bilayer (trilayer) preplating.

4. Conclusion

The present experiment and the previous results of Crowell and Reppy reveal a wealth of new phenomena in atomically layered superfluid ^{4}He films on graphite. Varying the substrate potential by preplating has proved to be a valuable tool to extract «universal» features of the behaviour of this system.

On the hydrogen bilayer and trilayer preplated surfaces we have studied there is no evidence for superfluidity in the first ^{4}He layer.

The second layer appears to condense into a $2D$ liquid at sufficiently low temperatures for a layer filling below 4 nm^{-2}. At higher coverages in this layer we believe it to be a uniform fluid. There is a rapid increase in the superfluid signal and T_c with coverage, much faster than that expected from KT theory. This may indicate a strong influence of the periodic substrate potential on superfluidity, which by extrapolation would completely suppress the superfluidity of a uniform fluid layer at a layer filling of order 0.6. However at completion of this second layer (first fluid layer) the transition temperature is close to the KT line, with a dead layer corresponding simply to the first solid layer.

On formation of the third layer, the period shift data show that the system consists of two superfluid layers atop an inert layer, which is believed to be solid for both preplatings. The increase of the superfluid transition temperature with coverage is now significantly slower than the KT line, but similar to behaviour seen on mylar substrates.

The superfluid transition temperature of the film would only appear to fit the expectation from KT theory at essentially one coverage, third layer promotion, for which the ^{4}He film consists of a single fluid layer atop a single solid layer atop the preplated substrate.

We believe that more theoretical work is required to understand the superfluid transition of a single fluid layer subject to a crystalline potential. It would also appear that the system of two fluid layers of ^{4}He would merit further study. To what extent are the layers, in particular the vortices, coupled? There are possible analogies with high T_c materials here. A future experimental objective is to attempt to grow a thick hydrogen film, and study the expected submonolayer superfluidity with torsional oscillator techniques.

Acknowledgements

We thank Chris Lusher for help with the data acquisition system and Marcio Siqueira for suggestions and comments. We should also especially like to thank P. Crowell, G. Mistura, P. S. Ebey, and O. E. Vilches for useful advices and discussions. Technical assistance was provided at various stages by John Taylor, Tony Wilkinson and Alan Betts. This work was supported by EPSRC (UK) and the Royal Society and partially supported by INTAS program (project 94-3416).

1. J. M. Kosterlitz and D. J. Thouless, *J. Phys.* **C6**, 1181 (1973), *ibid.* 7, 1046 (1974).
2. D. J. Bishop and J. D. Reppy, *Phys. Rev. Lett.* **40**, 1727 (1980), *Phys. Rev.* **B22**, 5171 (1980).
3. E. L. Andronikashvili, *Zh. Eksp. Teor. Fiz.* **16**, 780 (1946).
4. G. Agnolet, D. F. McQueeney, and J. D. Reppy, *Phys. Rev.* **B39**, 8934 (1989).
5. M. P. A. Fisher, P. B. Weichmann, G. Grinstein, and D. S. Fisher, *Phys. Rev.* **B40**, 546 (1989).
6. P. A. Crowell and J. D. Reppy, *Phys. Rev. Lett.* **70**, 3291 (1993), *Physica* **B197**, 269 (1994), *Phys. Rev.* **B53**, 2701 (1996).
7. P. Mohandas, C. Lusher, B. Cowan and J. Saunders, *J. Low Temp. Phys.* **89**, 613 (1992), P. Mohandas, C. P. Lusher, B. Cowan, and J. Saunders, *J. Low Temp. Phys.* **101**, 481 (1995).
8. G. Zimmerli, G. Mistura, and M. H. W. Chan, *Phys. Rev. Lett.* **68**, 60 (1991).

9. D. S. Greywall and P.A. Busch, *Phys. Rev.Lett.* **67**, 3535 (1991); D. S. Greywall, *Phys. Rev.* **B47**, 309 (1993).
10. E. Krotscheck, *Phys. Rev.* **B32**, 12453 (1991).
11. For a recent review see M. H. W. Chan, *Phase Transitions in Surface Films 2*, H. Taub, G. Torzo, H. J. Lauter, and S. C. Fain, Jr.(eds.) Plenum London (1991).
12. J. G. Brisson, J. C. Mester, and I. F. Silvera, *Phys. Rev.* **B44**, 12453 (1991).
13. P. J. Shirron and J. M. Mochel, *Phys. Rev. Lett.* **67**, 1118 (1991); J. M. Mochel and M. T. Chen, *Physica* B197, 278 (1994); M. T. Chen, J. M. Roesler, and J. M. Mochel, *J. Low Temp. Phys.* **89**, 125 (1992).
14. P. W. Adams and V. Rant, *Phys. Rev. Lett.* **68**, 2350 (1992).
15. R. N. J. Conradt, U. Albrecht, S. Herminghaus, and P. Leiderer, *Physica* **B194–196**, 679 (1994).
16. H. Wiechert, in: *Excitations in 2D and 3D Quantum Fluids*, A. F. G. Wyatt and H. J. Lauter (eds.), Plenum (1990).
17. P. S. Ebey and O. E. Vilches, *J. Low Temp. Phys.* **101**, 469 (1995); P. Ebey, *thesis*, University of Washington; O. E. Vilches, *private communication* (1995).
18. M. Bretz, J. G. Dash, D. C. Hickernell, E.O. McClean, and O. E. Vilches, *Phys. Rev.* **A8**, 1589 (1973).
19. M. Nielsen, J. P. McTague, and W. Ellerson, *J.. Phys. (Paris)* Colloq. **C4–10** (1997); H. J. Lauter, H. Godfrin, V. L. P. Franck, and H. P. Schildberg, *Physica* **B165–166**, 597 (1990).
20. H. J. Lauter, H. P. Schildberg, H. Godfrin, H. Wiechert, and R. Haensel, *Can. J. Phys.* **65**, 1435 (1987).
21. E. Cheng, M. W. Cole, W. F. Saam, and J. Treiner, *Phys. Rev.* **B46**, 13967 (1992).
22. P. A. Whitlock, G. V. Chester, and M. H. Kalos, *Phys. Rev.* **B38**, 2418 (1988).
23. J. G. Dash, *Phys. Rev. Lett.* **41**, 1178 (1978).
24. M. Schick and O. E. Vilches, *Phys. Rev.* **B48**, 9910 (1993).
25. B. E. Clements, E. Krotscheck, and H. J. Lauter, *Phys. Rev. Lett.* **70**, 1287 (1993); B. E. Clements, J. L. Epstein, E. Krotscheck, and M. Saarela, *Phys. Rev.* **B48**, 7450 (1993); B. E. Clements, *ESF Workshop on Quantum Fluids and Solids (Interfaces)*, unpublished (1994).
26. P. Mohandas et al. *Physica* **B194–196**, 55 (1994); V. A. Maidanov, N. P. Mikhin, N. F. Omelaenko, E. Ya. Rudavskii, A. S. Rybalko, V. K. Chagovets, V. A. Mikheev, P. Mohandas, B. P. Cowan, and J. Saunders, *Low Temp. Phys.* **20**, 527 (1994).
27. Obtained from R. Rentzsch, see R. Rentzsch, K. J. Friedland, A. N. Ionov, M. N. Mateev, I. S. Shlimak, C. Gladun, and H. Vinkelberg, *Phys. Status Solidi* **B137**, 691 (1986).
28. G. Zimmerli, *thesis*, Penn. State University.
29. Paroscientific Inc., Redmond, WA 98502 (USA).
30. The compressibility is $(\partial n/\partial \ln p)/k_B T n^2$, where n is the coverage and p the vapour pressure.
31. M. Siqueira, C. P. Lusher, B. P. Cowan, and J. Saunders, *Phys. Rev. Lett.* **71**, 1407 (1993) and unpublished heat capacity data.
32. R. Ray, J. Nyeki, G. A. Sheshin, B. Cowan, and J. Saunders *Czech. J. Phys.* **46** (Supp.S1), 422 (1996) has a brief report of this data, with a preliminary temperature scale.
33. E. Cheng, W. F. Saam, M. W. Cole, and J. Treiner, *J. Low Temp. Phys.* **92**, 11 (1993) and Ref. 12.
34. M. Wagner and D. M. Ceperley, *J. Low Temp. Phys.* **94**, 185 (1994).
35. We can now identify additional features in the dissipation and period shift below the superfluid transition, reported in J. Nyeki, R. Ray, V. Maidanov, M. Siqueira, B. Cowan, and J. Saunders, *J. Low Temp. Phys.* **101**, 279 (1995), as arising from such mode crossings between third sound resonances and the driven torsion mode. Note that this data was obtained with a different Grafoil sample to that used in the work reported in the present paper.
36. G. Zimanyi, P. A. Crowell, R. T. Scalettar, and G.G. Batrouni, *Phys. Rev.* **B50**, 6515 (1994).